Distribution of magnetic moment in Ni_3Al†

G. P. Felcher
Argonne National Laboratory, Argonne, Illinois 60439

J. S. Kouvel*
University of Illinois, Chicago, Illinois 60680
and Argonne National Laboratory, Argonne, Illinois 60439

A. E. Miller
University of Notre Dame, Notre Dame, Indiana 46556

(Received 21 April 1977)

The unpaired-spin density distribution in the weakly ferromagnetic ordered alloy Ni_3Al was determined by polarized-neutron diffraction measurements on a single-crystal sample of 75.9-at.% Ni. In this Cu_3Au-type structure, the local magnetization at a Ni site is similar in its radial dependence and cubic components (84% T_{2g}, 16% E_g) to that in pure nickel, though it is much smaller in magnitude. (The magnetic moments of the excess Ni atoms in Al sites are not significantly different from those at the Ni sites.) Consistent with the tetragonal environment of each Ni site, the magnetization distribution is further lowered in symmetry, resulting in an extreme situation in which the uncompensated spin is located predominantly in the lobes directed toward Ni neighbors and hardly at all in those directed toward Al neighbors. Comparison is made with the components of the Fermi-level density of states derived from a band calculation by Fletcher; the neutron-diffraction results are found to be qualitatively in accord.

INTRODUCTION

The magnetic behavior of the Cu_3Au-type ordered alloys $Ni_{3+x}Al_{1-x}$ has received in recent years a fair amount of attention.[1-7] Over the narrow composition range of this ordered phase, the various observed magnetic properties change enormously. From 73.5-at.% Ni (the lower composition limit) to 74.6-at.% Ni, the alloys are paramagnetic at all temperatures, while those richer in nickel up to 76 at.% (the upper composition limit) become ferromagnetic, with a maximum spontaneous moment of 10.4 emu/g (~$0.125\mu_B$/Ni atom) and a maximum Curie temperature of 71.5 °K.[1-3] Both the ferromagnetic moment and the Curie point vary smoothly over the composition range, with no observed anomalies at stoichiometry. This fact has prompted the consideration of these alloys as being magnetically uniform and thus in accordance with the Stoner collective-electron model. Confirmation of this interpretation was inferred from the extraordinarily large high-field differential susceptibility of the ferromagnetic alloys, as well as from the temperature dependence of their magnetization.[1-3] More recently, however, anomalies found in the low-temperature specific heat of Ni_3Al suggest the existence of magnetic inhomogeneities, which are not easily explained in terms of the Stoner model.[4-6] Measured isotherms of magnetization vs field above the Curie point, also indicate that the system is not magnetically uniform but possibly contains magnetic clusters.[4,7]

A more pertinent reason for our study of the magnetic-moment distribution within the Ni_3Al unit cell, stemmed from the fact that each Ni site in this cubic structure has a lower-symmetry (tetragonal) environment of Ni and Al neighbors. It seemed reasonable to expect that the distribution of the uncompensated spin around each Ni site would reflect this lower symmetry and thus manifest important electronic differences between Ni-Ni and Ni-Al bonds. This expectation was borne out most dramatically by the neutron-diffraction results which are presented in this paper and compared with recent energy-band calculations. The high-field differential susceptibility of Ni_3Al being very large, another purpose of our experiments was to see if any significant changes in the magnetic-moment distribution are produced by a large magnetic field. Since our sample was slightly off stoichiometry (75.9-at.% Ni), we obtained as a by-product an independent determination of the magnetic moment of the excess Ni atoms that enter substitutionally into the Al sites.

EXPERIMENTAL PROCEDURE

For our neutron diffraction work, a single-crystal sample was cut from an ingot containing several large grains. The large grains were grown from a slightly Ni-rich melt by a floating-zone technique utilizing radio-frequency heating and levitation. Each as-grown crystal showed a small amount of residual disordered-phase dendritic

structure, which was eliminated by a 48-h anneal at 1100 °C in a hydrogen atmosphere. The shaping of the sample was accomplished by spark cutting, spark planing, and etching, thus minimizing any atomic disordering produced by cold work damage. The chemical composition was determined by magnetic measurements on an ingot piece originally adjacent to the neutron diffraction sample. The values derived for the zero-temperature spontaneous magnetization (~10.1 emu/g) and the Curie point ($T_C \approx 70$ °K), when compared to published data,[2] are both consistent with an ordered Ni_3Al phase of ~75.9-at.% Ni. There was no evidence, either crystallographic or magnetic, for the coexistence of any disordered phase.

The sample was approximately a disk, 8 mm in diameter and 0.5 mm in its original thickness, which was sufficient for accurate diffraction measurements of the weak reflections. Its thickness was later reduced to 0.18 mm, which allowed the stronger reflections to be measured with less extinction effect. The diffraction experiments were performed with a polarized-neutron spectrometer at the CP-5 reactor of the Argonne National Laboratory. The sample was kept at liquid-helium temperature in a split-coil superconducting magnet whose field was vertical and normal to the scattering vector. Moreover, the sample was mounted on a goniometer with its disk axis, which was crystallographically ⟨110⟩, parallel to the horizontal axis of rotation. Thus the Bragg intensities could be measured by transmission in the (110) zone, for which extinction effects are minimal. The extinction was checked at the same reflection for different sample thicknesses and at equivalent reflections in and out of the transmission plane; under appropriate conditions, the extinction was practically absent. Most measurements were made with a 10-kOe field, in which the sample was a single ferromagnetic domain and the neutrons remained polarized in their flight path between the magnet coils. Some measurements were also made at 85 kOe.

For the geometry of our system, the magnetic field was applied along different crystallographic directions when different Bragg peaks were measured. However, since the magnetic anisotropy of Ni_3Al is quite low, the magnetic intensity of a given Bragg peak was found to be independent of the field direction. Standard polarized-neutron techniques were used, whereby measurements were made of the flipping ratio, $R = [(F_N + F_M)/(F_N - F_M)]^2$, for the various Bragg peaks, where F_N and F_M are, respectively, the nuclear and magnetic contributions to the structure factor.

DIFFRACTION DATA AND ANALYSIS

In our basic measurements on the Ni_3Al crystal, the flipping ratios were determined at 4.2 °K and 10 kOe for the eleven normal lattice lines and eleven superlattice lines of lowest index. The experimental values obtained for F_M/F_N are listed in Table I. The range of $(\sin\theta)/\lambda$ for these measurements (where 2θ is the scattering angle and $\lambda = 1.036$ Å, the neutron wavelength) was too restricted to allow a direct Fourier transformation of these data into a spatial distribution of magnetic moment. However, an analysis of these results in terms of an atomic model can yield various components of this distribution, and we have taken this route as follows.

The structure factors for the diffraction lines of Ni_3Al, assumed to have perfect Cu_3Au-type order, are expressible as

$$F(hkl) = b_{Al} + b_{Ni}^{I}(-1)^{h+k} + b_{Ni}^{II}(-1)^{k+l} + b_{Ni}^{III}(-1)^{l+h}, \quad (1)$$

where h, k, l, are the Miller indices for the cubic

TABLE I. Experimental values of the magnetic amplitudes, relative to the nuclear amplitudes, of the normal-lattice and superlattice lines for Ni_3Al (statistical errors in the last two digits are shown in parentheses). The superlattice results are compared with values calculated as described in the text.

hkl	$(\sin\theta)/\lambda$	F_M/F_N (exp)	hkl	$(\sin\theta)/\lambda$	F_M/F_N (exp)	F_M/F_N (calc)
111	0.2413	0.0220 (02)	001	0.1393	0.0462 (06)	0.0469
200	0.2786	0.0194 (02)	110	0.1970	0.0383 (06)	0.0387
220	0.3940	0.0125 (02)	201	0.3115	0.0260 (08)	0.0272
311	0.4621	0.0088 (03)	112	0.3412	0.0286 (11)	0.0288
222	0.4826	0.0088 (02)	003	0.4179	0.0269 (14)	0.0294
400	0.5572	0.0043 (03)	221	0.4179	0.0186 (11)	0.0181
331	0.6072	0.0053 (03)	310	0.4405	0.0119 (13)	0.0116
420	0.6230	0.0041 (02)	203	0.5022	0.0174 (14)	0.0166
422	0.6824	0.0041 (03)	312	0.5213	0.0083 (15)	0.0092
511	0.7238	0.0011 (03)	401	0.5744	0.0015 (20)	0.0011
333	0.7238	0.0033 (03)	223	0.5744	0.0102 (18)	0.0119

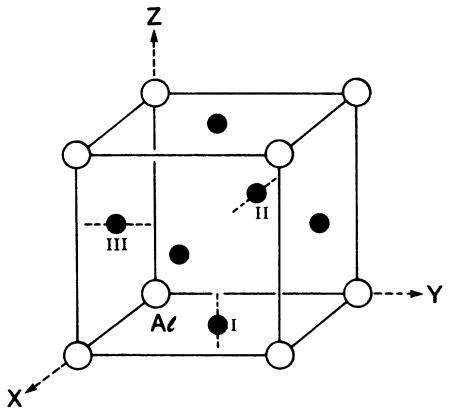

FIG. 1. Unit cell of Ni_3Al. The unique tetragonal axis of each Ni site is indicated.

cell and the b's represent the scattering amplitudes (nuclear or magnetic) for the atom sites situated as shown in Fig. 1. The expression clearly reflects the fact, illustrated in the figure, that the three types of Ni sites (I, II, III) have tetragonal point symmetry with mutually orthogonal unique axes of $\langle 001\rangle$-type, and that the Al site in each cell has cubic symmetry. The tetragonal character of the individual atom sites is averaged out in the normal-lattice lines (h, k, l all even or odd), for which

$$F_n = b_{\mathrm{Al}} + b^{\mathrm{I}}_{\mathrm{Ni}} + b^{\mathrm{II}}_{\mathrm{Ni}} + b^{\mathrm{III}}_{\mathrm{Ni}}, \tag{2a}$$

but not for the superlattice lines. The latter are distinguished by having Miller indices h_1, h_2, h_3, such that h_1+h_2 is even and h_1+h_3 is odd. Throughout the subsequent discussion, we use the labeling: $h_1=h$, $h_2=k$, $h_3=l$. Thus the structure factor of the superlattice lines is

$$F_s = b_{\mathrm{Al}} + b^{\mathrm{I}}_{\mathrm{Ni}} - b^{\mathrm{II}}_{\mathrm{Ni}} - b^{\mathrm{III}}_{\mathrm{Ni}}. \tag{2b}$$

The nuclear contribution (F_N) to the structure factors has been calculated from the published values of $b_{\mathrm{Ni}}=1.03$ and $b_{\mathrm{Al}}=0.345$ (in 10^{-12} cm), under the assumption that in our nonstoichiometric Ni_3Al crystal the excess Ni atoms occupy Al sites at random. Then, from the measured flipping ratio R, the magnetic contribution (F_M) for the various reflections is obtained; its values relative to F_N are listed in Table I. Since the Al atoms carry no magnetic moment, these results for the magnetic structure factors contain information specific to the localized unpaired-spin density of the Ni atoms in the alloy, which presumably has $3d$ character.

To extract this information, we allow that the tetragonal crystal field at each site splits the $3d$ band into four (presumably overlapping) subbands corresponding to electron distributions of $A_1(z^2)$, $B_2(x^2-y^2)$, $B_1(xy)$, and $E(xz, yz)$ symmetry, where the local unique axis is taken as z. Hence, the spin-only magnetic form factor for the Ni(I) atoms, located as shown in Fig. 1, may be written[8,9]

$$f^{\mathrm{I}}_{\mathrm{Ni}} = \langle j_0\rangle - \tfrac{10}{7}x_1 P_2^0(\beta)\langle j_2\rangle + \tfrac{18}{7}x_2 P_2^0(\beta)\langle j_4\rangle + \tfrac{15}{8}x_3 \sin^4\beta\cos 4\alpha\langle j_4\rangle, \tag{3}$$

where

$$x_1 = A_1 + \tfrac{1}{2}E - B_1 - B_2,$$
$$x_2 = A_1 - \tfrac{2}{3}E + \tfrac{1}{6}B_1 + \tfrac{1}{6}B_2,$$
$$x_3 = B_2 - B_1.$$

A_1, B_2, B_1, and E are the fractional magnetizations of the different subbands, α and β are the Euler angles of the momentum transfer $\vec{k}$ referred to the local unique axis (z in this case), the P's are spherical harmonics, and the $\langle j\rangle$'s are Bessel transforms of the $3d$ radial density distribution. Combining Eq. (3) with analogous expressions for $f^{\mathrm{II}}_{\mathrm{Ni}}$ and $f^{\mathrm{III}}_{\mathrm{Ni}}$ in the manner indicated in Eqs. (2a) and (2b), we obtain for the normal-lattice and superlattice magnetic structure factors,

$$F_n/\mu_{\mathrm{Ni}} = 3\langle j_0\rangle + 3(\tfrac{3}{2}E_g - T_{2g})A_{hkl}\langle j_4\rangle, \tag{4a}$$

$$F_s/\mu_{\mathrm{Ni}} = -\langle j_0\rangle - \tfrac{10}{7}x_1 B_{hkl}\langle j_2\rangle + \tfrac{9}{14}x_2 C_{hkl}\langle j_4\rangle - \tfrac{15}{4}x_3 D_{hkl}\langle j_4\rangle, \tag{4b}$$

with

$$E_g = A_1 + B_2, \quad T_{2g} = B_1 + E, \quad E_g + T_{2g} = 1,$$
$$A_{hkl} = 1 - 5(h^2k^2 + h^2l^2 + k^2l^2)/r^4,$$
$$B_{hkl} = 3l^2/r^2 - 1,$$
$$C_{hkl} = 5(7h^2k^2 + h^2l^2 + k^2l^2 + l^4)/r^4 - 4,$$
$$D_{hkl} = 3(h^2k^2 - h^2l^2 - k^2l^2 + l^4/3)r^4,$$

where l is chosen as the unique index, $r^2 = h^2 + k^2 + l^2$, and μ_{Ni} is the magnetic moment per Ni atom. Note that Eq. (4a) involves only the cubic-field distributions, E_g and T_{2g}, since F_n averages the scattering amplitudes of the three Ni atoms with mutually orthogonal tetragonal axes; any departure from sphericity ($\frac{3}{2}E_g \neq T_{2g}$) is contained in its $\langle j_4\rangle$ term. Any further lowering of symmetry from cubic to tetragonal ($A_1 \neq B_2$, $E \neq 2B_1$) is reflected only in F_s, the $\langle j_2\rangle$ term in Eq. (4b) becoming nonzero and the $\langle j_4\rangle$ terms changing in magnitude.

For an approximate estimate of the cubic-field magnetization distributions in our Ni_3Al crystal, the magnetic structure factor results for the normal-lattice (fcc) lines given in Table I were compared with those published[10] for pure nickel. Since the lattice spacings in Ni and Ni_3Al are slightly different, the results for Ni were adjusted so as to bring them to the same values of $(\sin\theta)/\lambda$. This adjustment was accomplished for various points

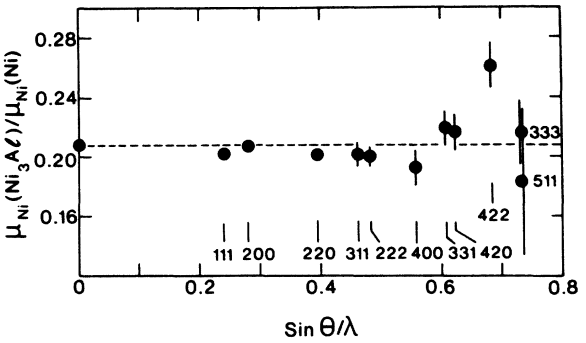

FIG. 2. Ratio of the average magnetic moment per Ni atom in Ni_3Al to that in pure nickel from various fcc-lattice reflections.

on a continuous form-factor curve[11] by means of the parameters deduced by Mook.[10] The ratio of the magnetic structure factors of the two materials at each fcc reflection, divided by the ratio of their Ni concentrations (i.e., 0.759) is plotted against $(\sin\theta)/\lambda$ in Fig. 2. This quantity should have a constant value (equal to the ratio of the average moments per Ni atom) if the cubic-field magnetization distributions in the two materials are the same. The figure shows that this is very nearly the case for all the measured reflections. Thus the radial or spherically averaged part of the form factor of Ni in Ni_3Al is quite similar to that in pure nickel and is predominantly of $3d$ character, as assumed in the analysis of the form factor [Eq. (3)]. Even the cubic occupation numbers, $E_g = 19\%$ and $T_{2g} = 81\%$, previously deduced for the unpaired-spin density distribution in nickel,[10] apply fairly closely to Ni_3Al. These findings are remarkable in themselves in view of the very large difference between the ferromagnetic moments per Ni atom of the two materials.

A more direct analysis of the magnetic-structure-factor results for Ni_3Al requires the fitting of the data with a model form factor. This is usually the $3d$ form factor for the magnetic ion of valence 2+, as obtained by a Hartree-Fock calculation. This model form factor has spin-only character and must therefore be adjusted; an orbital contribution must be added in the amount prescribed by the gyromagnetic ratio of the material. Furthermore, a conduction-electron contribution must also be added in the amount necessary to achieve consistency between the neutron scattering and magnetization data.[11] However, this procedure is not possible for Ni_3Al since the two corrections are not known, and we therefore proceeded as follows.

TABLE II. Experimental asphericity parameters and magnetic moment per excess Ni atom (in Al sites) in $Ni_{0.759}Al_{0.241}$.

$x_1 = A_1 + \frac{1}{2}E - B_1 - B_2$	0.34 ± 0.03
$x_2 = A_1 - \frac{2}{3}E + \frac{1}{6}B_1 + \frac{1}{6}B_2$	-0.44 ± 0.04
$x_3 = B_2 - B_1$	0.09 ± 0.08
$(\frac{3}{2}E_g - T_{2g})_s$	-0.54 ± 0.12
$(\frac{3}{2}E_g - T_{2g})_n$	-0.52 ± 0.03
$\mu_{Ni}^{(Al)}$	$(0.13 \pm 0.04)\mu_B$

We began with the normal-lattice reflections and removed the aspherical components of F_n [represented by the last term in Eq. (4a)], using calculated[12] Hartree-Fock values of $\langle j_4 \rangle$ and adjusting the parameter $\frac{3}{2}E_g - T_{2g}$ until the corrected points fell on a smooth curve. The optimum value of this parameter is shown in Table II. The curve thus obtained (see Fig. 3) was allowed to define an effective $\langle j_0 \rangle$, which presumably contains orbital as well as spin contributions to the spherical polarization. Using $\langle j_0 \rangle_{eff}$ to assign values to the spherical components of the magnetic structure factors for the superlattice peaks, we compared our experimental results against the parametric expression,

$$F_s/\mu_{Ni} = x_0\langle j_0\rangle_{eff} - \tfrac{10}{7}x_1 B_{hkl}\langle j_2\rangle + \tfrac{9}{14}x_2 C_{hkl}\langle j_4\rangle - \tfrac{15}{4}x_3 D_{hkl}\langle j_4\rangle , \quad (5)$$

where

$$x_0 = (c\mu_{Ni}^{(Al)} - \mu_{Ni}^{(Ni)})/\mu_{Ni}^{(Ni)} .$$

This expression is an obvious modification of Eq.

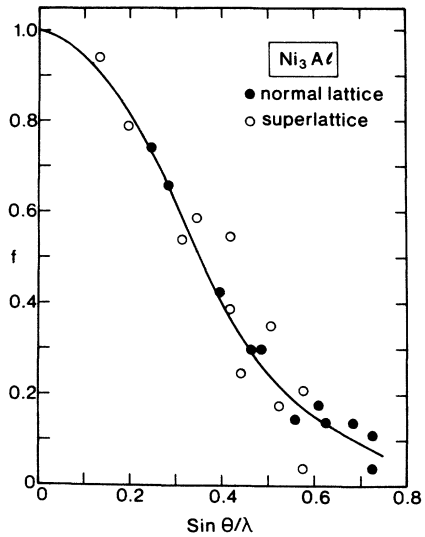

FIG. 3. Form factor of Ni_3Al. Closed circles, normal lattice lines; open circles, superlattice lines. The curve represents an interpolated spherical form factor for Ni in Ni_3Al. Error bars are omitted for clarity.

TABLE III. Cubic and tetragonal components of the magnetic moment distribution in Ni_3Fe (from Ref. 9), in nickel (from Ref. 10), and in Ni_3Al (present work). The uncertainties indicated for the tetragonal components are not independent. Relative density of states at the Fermi level for the various $3d$ subbands of Ni_3Al (from Ref. 17).

	μ_{Ni}	Ni_3Fe $0.68\mu_B$	Nickel $0.61\mu_B$	Ni_3Al $0.12\mu_B$	Ni_3Al $N(E_f)$
E_g	$A_1(3z^2-r^2)$	8		7±3	4
		26	19±1	16±2	25
	$B_2(x^2-y^2)$	18		9±4	21
T_{2g}	$B_1(xy)$	18		4±4	6
		74	81±1	84±2	75
	$E(xz,yz)$	56		80±3	69

(4b) for compounds of nonstoichiometric composition $Ni_3(Ni_cAl_{1-c})$, in which $\mu_{Ni}^{(Ni)}$ and $\mu_{Ni}^{(Al)}$ are the average moments of Ni atoms on Ni and Al sites, respectively; for our crystal, $c \approx 0.035$. The procedure thus followed is justified since, even in a more complete treatment, the largest corrections to the spin-only Hartree-Fock form factor involve only the spherical $\langle j_0 \rangle$ term. The aspherical terms are merely scaled up or down by a numerical factor close to unity (0.92 for pure nickel), which does not affect significantly the relative populations of the $3d$ levels. The x-parameter values that gave the best least-square fit to the experimental results for F_s, the magnetic structure factors for the superlattice peaks, are presented in Table II. The calculated values of F_s are listed in Table I, next to the corresponding experimental values.

As indicated in Table II, the value for $\mu_{Ni}^{(Al)}$ was not determined very accurately (from x_0) due to the uncertainty about the imperfect stoichiometry of our crystal, but it does not appear to differ greatly from the $\mu_{Ni}^{(Ni)}$ value of $0.125\mu_B$. In principle, the other three parameters (x_1, x_2, x_3), together with the normalization condition ($A_1+B_2+B_1+E=1$), can be used directly to evaluate the occupation numbers of the four individual tetragonal-field distributions. However, such a procedure would result in very large errors, which stem from the poor determination of x_3. This is evidenced by the $\frac{3}{2}E_g - T_{2g}$ parameter determined from $\frac{1}{4}(6x_2+5x_3)$, which is compared in Table II with the value of this parameter deduced from our F_n results, as described earlier. Although the two values are in fair agreement, the latter is clearly much more accurate. Hence, as a better alternative, we evaluated the individual occupation numbers from the weighted average of the two $\frac{3}{2}E_g - T_{2g}$ values, plus x_1, x_2, and the normalization condition. Our results are presented in Table III and will be discussed in the following section.

The flipping ratios for six superlattice lines were also measured in a field of 85 kOe, again at 4.2 °K, where the magnetization of our Ni_3Al crystal is 1.165 times its magnitude at 10 kOe. Our aim was to see if this increase in the total magnetization is accompanied by any change in the unpaired-spin density distribution. Such a change would be manifested in different relative increases of magnetic structure factors for different reflections. As demonstrated in Fig. 4, this was not found to be the case; within the error limits indicated in Table III, there was no significant readjustment of the tetragonal-field distribution numbers.

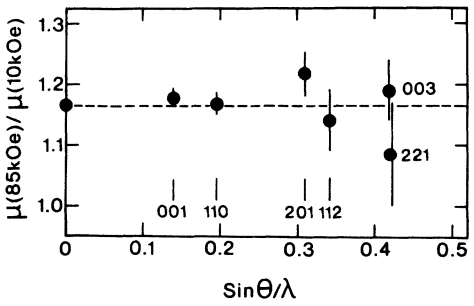

FIG. 4. Ratio of the magnetic amplitude for Ni_3Al in a field of 85 kOe to that in 10 kOe, for several superlattice reflections.

DISCUSSION

To start with, our experiments have shown that the excess Ni atoms in our off-stoichiometric Ni_3Al sample have a magnetic moment that is not significantly different from that of the other Ni atoms. It was assumed that the excess Ni atoms reside at random on the Al sites and that the Ni sites are fully occupied by the other Ni atoms. This assumption was validated experimentally by the relative intensities of the superlattice reflections compared to the normal-lattice reflections; a modest amount of atomic disorder (~1%) would not alter this interpretation appreciably. Since a Ni atom on an Al site has only Ni nearest neighbors, it would be tempting to assign to it a magnetic moment comparable to that in pure nickel and to consider it as the nucleus of a "giant magnetization cloud" of the type attributed to Ni-Cu and other disordered alloys.[13] Such a picture could explain the magnetic inhomogeneities deduced from specific-heat and susceptibility measurements[4-7] and would relate closely (though not exactly) to the

formation of giant moments in Ni_3Al that is doped with iron impurities,[2,14] Recently, however, a diffuse neutron scattering experiment, on $Ni_{0.76}Al_{0.24}$ and the stoichiometric alloy, revealed that only a very small intensity can be associated with any spatial fluctuations of the magnetization.[15] This experiment specifically rules out magnetic clusters of diameter less than ~40 Å and of concentration c and moment μ such that $c^{1/2}\mu > 0.2\ \mu_B$/cluster. It does not quite rule out the picture described above, but our present measurements disallow this picture completely. Thus a different or subtler origin must be sought for the susceptibility and specific-heat anomalies observed in Ni_3Al.

A second and more intrinsic result of our polarized neutron work on Ni_3Al is the determination of the asphericity of the local ($3d$) magnetization distribution around each Ni atom. Most immediately, we have found that the cubic-field components of this distribution (T_{2g} and E_g) are very close in relative magnitude to those in pure nickel, though they are much smaller in absolute magnitude, even in a large magnetic field (85 kOe). More detailed analysis of our data has revealed a further splitting of this distribution into tetragonal-field components, the most striking feature of which is that the B_1 component associated with the $3d$ electrons in the bonds between a Ni atom and its Al nearest neighbors contains essentially no uncompensated spin. A similar but less drastic depletion of the B_1 component of the moment density distribution was previously found in the isomorphically ordered alloy Ni_3Fe,[9] as shown in Table III. However, this table also shows that the cubic-field components in Ni_3Fe correspond to a more spherical magnetization distribution than in Ni_3Al or pure nickel. Both of these qualitative features have also been seen in the $5d$-moment distribution in Pt_3Mn,[8] which also has a Cu_3Au-type structure.

The aspherical distribution of uncompensated spin in Ni_3Al can also be compared with the density of $3d$ states at the Fermi level, which we determined from a complete band calculation carried out by Fletcher[16] for paramagnetic Ni_3Al. From the wave vectors for the tight-binding wave functions at and near the Fermi energy (i.e., within ±0.013 Ry),[17] we evaluated the density of states for the individual $3d$ subbands, which are split by a tetragonal field. The results are presented in Table III. A major aspect of these results is the essential absence of the B_1 subband, which lies almost completely below the Fermi level. This immediately explains the extremely small value we have found for the B_1 component of the uncompensated spin. A quantity that is much more difficult to obtain accurately from the band calculations is the relative Fermi-level density of states of the T_{2g} and E_g subbands, which depends very sensitively on the averaging of the potential outside the Wigner-Seitz radii. Thus it is gratifying that the calculated results indicate a preponderance of T_{2g} states over E_g states at the Fermi level. From the exchange splitting of these subbands, one can expect a correspondingly preponderant T_{2g} component of magnetic moment, which is what our neutron diffraction results have shown. Hence, in summary, there appears to be a broad agreement between our experimental results for the various components of the magnetization distribution in Ni_3Al and the corresponding components of the Fermi-level density of states derived from the band calculation.

ACKNOWLEDGMENTS

We wish to thank Dr. G. C. Fletcher for sending us his unpublished results for the Fermi-level wave vectors of Ni_3Al. We are also grateful to Dr. T. O. Brun for his help in the initial experiments and to Dr. D. D. Koelling for enlightening discussions of the band structures of Cu_3Au-type ordered materials.

---

†Performed under the auspices of the U. S. ERDA.
*Supported in part by the NSF.

[1]F. R. De Boer, C. J. Schinkel, and J. Biesterbos, Phys. Lett. A 25, 606 (1967).
[2]F. R. De Boer, Ph.D. thesis (University of Amsterdam, 1969) (unpublished).
[3]F. R. De Boer, C. J. Schinkel, J. Biesterbos, and S. Proost, J. Appl. Phys. 40, 1049 (1969).
[4]C. G. Robbins and H. Claus, AIP Conf. Proc. 5, 527 (1971).
[5]R. W. Jones, G. S. Knapp, and C. W. Chu, AIP Conf. Proc. 10, 1618 (1972).
[6]W. de Dood and P. F. de Chatel, J. Phys. F 3, 1039 (1973).
[7]A. Parthasarathi and P. A. Beck, AIP Conf. Proc. 29, 282 (1975).
[8]B. Antonini, F. Lucari, F. Menzinger, and A. Paoletti, Phys. Rev. 187, 611 (1969). In the nomenclature for the tetragonal-field components, we have followed that used in this reference.
[9]J. W. Cable and E. O. Wollan, Phys. Rev. B 7, 2005 (1973); 8, 3487 (1973).
[10]H. A. Mook, Phys. Rev. 148, 496 (1966).
[11]R. M. Moon, Int. J. Magn. 1, 219 (1971).
[12]R. E. Watson and A. J. Freeman, Acta Crystallogr. 14, 27 (1961).
[13]T. J. Hicks, B. Rainford, J. S. Kouvel, G. G. Low, and J. B. Comly, Phys. Rev. Lett. 22, 531 (1969); A. Amamou, F. Gautier, and B. Loegel, J. Phys. (Paris) 35, C4-217 (1974); W. C. Muellner and J. S.

Kouvel, Phys. Rev. B 11, 4552 (1975).
[14]P. C. Ling and T. J. Hicks, J. Phys. F 3, 697 (1973).
[15]J. W. Cable, H. R. Child, and J. B. Comly, Oak Ridge Natl. Lab. Solid State Div. Annual Prog. Rep. (1973), p. 106.
[16]G. C. Fletcher, Physica (Utrecht) 56, 173 (1971); 62, 41 (1972).
[17]G. C. Fletcher (private communication).